THE AFTERGLOW OF MASSIVE BLACK HOLE COALESCENCE

MILOŠ MILOSAVLJEVIĆ[1] AND E. S. PHINNEY[1]

[1]Theoretical Astrophysics, California Institute of Technology, Mail Code 130-33, 1200 East California Boulevard, Pasadena, CA 91125.

Draft version September 1, 2018

ABSTRACT

The final merger of a pair of massive black holes in a galactic nucleus is compelled by gravitational radiation. Gravitational waves from the mergers of black holes of masses $(10^5 - 10^7)(1+z)^{-1} M_\odot$ at redshifts of $1 - 20$ will be readily detectable by the *Laser Interferometer Space Antenna*, but an electromagnetic afterglow would be helpful in pinpointing the source and its redshift. Long before the merger, the binary "hollows out" any surrounding gas and shrinks slowly compared to the viscous timescale of a circumbinary disk. The inner gas disk is truncated at the radius where gravitational torque from the binary balances the viscous torque, and accretion onto the black holes is diminished. Initially, the inner truncation radius is able to follow the shrinking binary inward. But eventually the gravitational radiation timescale becomes shorter than the viscous timescale in the disk, leading to a merged black hole surrounded by a hollow disk of gas. We show that the subsequent viscous evolution of the hollow, radiation pressure-dominated disk will create an $\sim 10^{43.5}(M/10^6 M_\odot)$ergs s^{-1} X-ray source on a timescale $\sim 7(1+z)(M/10^6 M_\odot)^{1.32}$ yr. This justifies follow-up monitoring of gravitational wave events with next-generation X-ray observatories. Analysis of the detailed light curve of these afterglows will yield new insights into the subtle physics of accretion onto massive black holes.

Subject headings: accretion, accretion disks — black hole physics — quasars: general — X-rays: galaxies

1. INTRODUCTION

Evidence is mounting that galactic spheroids contain massive black holes (MBHs) in their nuclei. When two galaxies merge, their MBHs form a binary in the nucleus of the new galaxy (Begelman, Blandford, & Rees 1980). The binary interacts with its stellar and gaseous environment and with other MBHs that collect in the same nucleus in multiple mergers. These interactions torque the binary and extract its orbital angular momentum and energy. The binary can thus be rendered so compact that gravitational radiation (GR) carries away the remaining orbital energy, inducing coalescence. For binaries with masses $M = M_1 + M_2 \lesssim 10^7 M_\odot$, the gravitational slingshot ejection of stars is sufficient to guarantee coalescence in a Hubble time (Milosavljević & Merritt 2003). GR emitted by these binaries shortly before and during coalescence will be detected by the space-based gravitational wave detector *Laser Interferometer Space Antenna* (*LISA*).[1] The coalescence of isolated black holes in general relativity is not accompanied by observable electromagnetic (EM) emission. We here show that circumbinary gas can lead to a delayed EM afterglow.

Of interest to *LISA* are mergers of binaries with masses $M < 10^7 M_\odot$ of arbitrary mass ratio $q \le 1$. There is abundant evidence for dense gas in galactic nuclei. Geometrically thin molecular disks have been detected in water maser emission in Seyfert galaxies (e.g., Miyoshi et al. 1995; Greenhill et al. 2003). The Galactic nucleus contains a $4 \times 10^6 M_\odot$ MBH surrounded by an $\sim 10^4 M_\odot$ molecular gas torus (e.g., Jackson et al. 1993). Massive accretion disks must be present in quasars and narrow-line Seyfert I nuclei to explain their luminosities.

In general, the specific angular momentum of inflowing gas exceeds that of the binary, while the gas temperature is below the virial temperature $GM\mu m_p/2ak$, where μ is the mean molecular weight in units of the proton mass m_p, a is the binary's semimajor axis, and k is the Boltzmann constant. The sub-virial gas settles into a ro-

tationally supported, geometrically thin circumbinary disk. If the disk is inclined with respect to the binary's orbital plane, the quadrupole component of the binary's gravitational potential causes differential precession and the warping of the disk. As in the Bardeen & Petterson (1975) mechanism, the warp dissipates viscously, resulting in a disk in the binary's orbital plane (Larwood & Papaloizou 1997; Ivanov, Papaloizou, & Polnarev 1999).

The disk is truncated at an inner edge where gravitational torques and viscous stresses balance (e.g., Artymowicz & Lubow 1994). Surface density in the hollowed region is much smaller than in the disk (e.g., Günther, Schäfer, & Kley 2004). While material does peel off the inner edge and flow across the hole (Artymowicz & Lubow 1996), the accretion rate for moderate mass ratios ($q \gtrsim 0.01$) is only a fraction ($\lesssim 10\%$) of the rate at which the disk would be accreting without being torqued by the binary (Lubow, Seibert, & Artymowicz 1999). As the binary's semimajor axis decays owing to stellar or gas dynamical processes (including angular momentum extraction by the circumbinary disk itself), the disk's inner edge spreads inward viscously while maintaining an approximately constant ratio of inner edge radius to semimajor axis, $r_{edge}/a \sim 2$. In the final stages of in-spiral, however, the time for decay of the semimajor axis is set by GR and decreases rapidly with a (equation 1). When this becomes shorter than the (viscous) time for the inner edge of the disk to spread inward, the binary continues toward merger while the disk structure remains frozen (Armitage & Natarajan 2002). This was also noted by Liu, Wu, & Cao (2003), who suggested that the formation of an inner hole in the disk preceding MBH coalescence causes the interruption of jet activity in double-double radio galaxies.

Vertical support in the central parts of MBH accretion disks is dominated by radiation pressure, while opacity is dominated by electron scattering. The Shakura & Sunyaev (1973) α-disks in this regime are thermally and viscously unstable (Lightman & Eardley 1974) if viscous stresses scale with to-

tal pressure. However, they are stable if the stresses scale with the gas pressure alone (Sakimoto & Coroniti 1981). Such a scaling can occur (Turner 2004) if the distance photons diffuse per orbit is about equal to the scale of magnetic fields produced by the magnetorotational instability (MRI; Balbus & Hawley 1991) that facilitates angular momentum transport. The radiation then partly decouples from the turbulence driven by the MRI (Turner et al. 2003). These disks are clumpy and porous to the radiation produced within (Begelman 2002 and references therein).

We here describe the observable signatures of such circumbinary disks in MBHs. In § 2, we present a scenario for the combined evolution of an MBH binary and its circumbinary accretion disk immediately preceding coalescence. In § 3, we discuss observable signatures.

2. A MODEL FOR BINARY-DISK EVOLUTION

In the early stages of the GR-driven orbital evolution, the binary orbit is circularized by GR. Furthermore, unless $q \ll 1$, the timescale (Peters 1964)

$$t_{gr} \equiv \frac{a}{da/dt} = \frac{5}{64} \frac{c^5 a^4}{G^3 M^3} \frac{(1+q)^2}{q}. \qquad (1)$$

on which the binary's semimajor axis a decays because the emission of GR greatly *exceeds* the viscous timescale $t_{visc} = (2/3)r^2/\nu(r)$ for $r \sim a$. For realistic disks (see below), the effective kinematic viscosity ν is a weak function of radius, so $t_{visc} \propto r^2$ approximately. Thus, any gas *inside* the binary orbit should long ago have been accreted (for $r \ll a$) or expelled (for $r \sim a$), leaving the MBHs in a gas-free "donut hole."[2]

Gas outside the binary will attempt to accrete but be prevented by torques from the binary (§ 1). The inner edge of the disk lies at $r_{edge} = 2\lambda a$, where $\lambda > 0.5$ is a parameter of order unity. In this regime, the viscous torque in the disk $3\pi r^2 \nu \Sigma \Omega$ is constant with radius (e.g., Pringle 1991). Here Σ is the surface density and $\Omega = (GM/r^3)^{1/2}$ is the local angular velocity. As the binary shrinks, the inner parts of the circumbinary disk pass through a time sequence of nonaccreting, constant torque configurations. In the outer parts of the disk it can occur that $t_{gr} < t_{visc}(r)$, where r is a radius in the disk. Then material outside r loses viscous causal connection with the inner edge and decouples from the binary torque.

Since $t_{gr} \propto a^4$, while the viscous timescale at r_{edge} approximately scales as $t_{visc} \propto a^2$, the shrinking binary/disk system eventually reaches a state in which $t_{gr} < t_{visc}(r_{edge})$, i.e., the whole disk has decoupled from the rapidly shrinking binary. The inner parts of the disk begin to evolve as a standard, zero-torque disk. When the inner edge decouples, the radial profile closely resembles the non-accreting disk with a sharp edge. The inner edge reaches the center in time $t_{sh} \sim \beta t_{visc}(r_{edge})$, where $\beta \equiv \max\{0.1, [d\ln\Sigma/d\ln r(r_{edge})]^{-1}\}$. The factor 0.1 is appropriate for an infinitely sharp disk (Lynden-Bell & Pringle 1974). To estimate t_{sh} and the self-consistent a for which $t_{gr} \sim t_{sh}$, we must determine the internal structure and viscosity of the inner disk at the time of decoupling, to which problem we turn now.

In the stable α-model, the kinematic viscosity is given by $\nu \sim \frac{2}{3}\alpha_{gas}P_{gas}/\rho\Omega$, where $P_{gas} = \rho kT/\mu m_p$ is the gas pressure, and ρ is the density. To prevent confusion, we define α_{gas}, related to the usual definition via $\alpha_{gas}P_{gas} = \alpha P_{total}$, where

$P_{total} = P_{rad} + P_{gas} + P_{mag}$ is the sum of the radiation, gas, and magnetic pressures. In a simulation of one such accretion disk, Turner (2004) measures $\alpha = 0.0013$ and $P_{rad}/P_{gas} = 14$ while $P_{mag} \ll P_{rad}$, implying that $\alpha_{gas} \approx 0.02$ in his simulation. We defer modeling the detailed vertical structure of the disk to a follow-up paper; relations presented below are approximate.

The rate of local dissipation per unit area of the disk equals $\mathcal{Q} \sim (9/4)\nu\Sigma\Omega^2$. When we ignore horizontal advection, the flux $F = \mathcal{Q}/2$ must be emitted from each surface. If the surface is emitting as a blackbody, the flux equals $F_{bb} = 4\sigma T^4/3\tau$, where T is the midplane temperature, τ is the total optical depth, and σ is the Stefan-Boltzmann constant. The spectrum differs from that of a blackbody since the photons at different frequencies are thermalized at different depths. The modified, "graybody" spectrum has emergent flux $F_\nu \sim \pi\epsilon_\nu^{1/2}(1+\epsilon_\nu^{1/2})^{-1}B_\nu$, where B_ν is the Planck function and $\epsilon_\nu = \kappa_{abs,\nu}/(\kappa_{abs,\nu} + \kappa_{es})$ is the ratio of the absorption to the total opacity, and κ_{es} is the electron scattering opacity. The quantities B_ν and ϵ_ν are evaluated at the bottom of the thermalization photosphere (TP); we denote the temperature and the density there by T_ν and ρ_ν, respectively.

The scale height of the photosphere is given by $h_\nu \sim [\gamma P_{rad}(T_\nu)/\rho_\nu]^{1/2}/\Omega$, where $\gamma \approx 4/3$ is the adiabatic index. We set the absorption opacity equal to the (mainly bound-free) opacity $\kappa_\nu \approx 3 \times 10^{26}g_{bf}\rho T^{-7/2}\xi^{-3}(1-e^{-\xi})$ cm^2 g^{-1}, with ρ and T in cgs, where $\xi \equiv h\nu/kT$, h is the Planck constant, and $g_{bf} \sim 1$ is the gaunt factor (κ_ν is the free-free opacity scaled up by the ratio of the bound-free to the free-free Rosseland mean opacities at solar metallicity). By definition, the effective optical depth $\sim (\kappa_{abs,\nu}\kappa_{es})^{1/2}\rho_\nu h_\nu = 1$ at the bottom of TP. This is solved for ρ_ν, which we substitute back in κ_{abs} to find that $\epsilon_\nu^2 = 1.4 \times 10^{42}g_{bf}\Omega^2 T_\nu^{-15/2}\xi^{-3}(1-e^{-\xi})$. To estimate the degree to which blanketing by the TP modifies the integrated emitted flux, we evaluate ϵ_ν at the Wien frequency ($\xi \approx 2.8$). We relate T_ν to the midplane temperature via $T_\nu = \tau^{-1/4}T$, where τ is the electron scattering optical depth between the photosphere and the midplane. This yields

$$F_{gb} \equiv \int_0^\infty F_\nu d\nu \sim \frac{4\sigma T^4}{3\tau}\frac{\sqrt{\epsilon}}{1+\sqrt{\epsilon}} \sim \frac{9}{8}\nu\Sigma\Omega^2, \qquad (2)$$

where $\epsilon \sim 2.5 \times 10^{20}\Omega\tau^{15/16}T^{-15/4}$ and the last approximate equality in equation (2) follows from identifying F_{gb} with half of the power generated in the disk. The disk edge has $\epsilon < 1$ at decoupling, resulting in a higher midplane temperature than in the blackbody disk.

The optical depth is given by $\tau = \theta\kappa\Sigma$, where κ is the opacity (electron scattering $\kappa_{es} \approx 0.4$ cm^2 g^{-1}, or Kramer's $\kappa_{abs} \approx 1.6 \times 10^{24}\rho T^{-7/2}$ g^{-1}) and $\theta \leq 1$ is a "porosity" correction factor. We introduce θ to account for the shortened effective optical depth in an inhomogeneous disk in which radiation escapes through low-density domains. The correction can also be used to approximate disks in which a fraction of the turbulent magnetic energy is dissipated in surface layers (Miller & Stone 2000) or in the presence of photon-bubble instability (Gammie 1998). We estimate that $\theta \approx 0.2$ in Turner (2004).

The surface density is thus far unspecified. One (admittedly artificial) way to parametrize Σ is to fix the accretion rate $\dot{M} \equiv 3\pi\nu\Sigma$ that the disk would have at its inner edge if it contained a single black hole instead of a binary (the disk is not in viscous equilibrium, and the accretion rate varies with radius).

---

[2] This is in contrast to the $q \ll 1$ case considered by Armitage & Natarajan (2002), who assumed that there was still gas accreting onto the black holes.

The accretion rate can be expressed in units of the Eddington rate $\dot{M}_{\mathrm{edd}} \equiv 4\pi GMm_{\mathrm{p}}/\eta c\sigma_{\mathrm{T}}$, where $\eta \sim 0.1$ is the radiative efficiency and σ_{T} is the Thomson cross section; $\dot{M}_{\mathrm{edd}}$ should not be confused with the *local* Eddington limit at the disk edge. We define the dimensionless parameter $\dot{m} \equiv \dot{M}/\dot{M}_{\mathrm{edd}}$. There is no a priori requirement for $\dot{m} \leq 1$; in fact, following decoupling the accretion rate will likely be the largest anywhere among black holes of the same mass. The surface density is thus parametrized via

$$\nu\Sigma = \frac{4}{3}\frac{GMm_{\mathrm{p}}}{\eta c\sigma_{\mathrm{T}}}\dot{m}. \qquad (3)$$

Another way to characterize the surface density is via the total mass of the disk M_{disk} (see Table 1), out to the radius where the temperature falls below 10^4 K (see below).

To determine the disk properties at the time of decoupling, we equate t_{sh} with t_{gr}, which with the expression for the viscosity determines the midplane temperature near the disk edge in terms of the semimajor axis. This is then used in equations (2) and (3) to solve for the semimajor axis a, the edge surface density Σ, and the edge midplane temperature T at decoupling. Self-consistent solutions are in the radiation pressure-dominated and electron scattering-dominated regime. The results are summarized in Table 1. We have defined $\alpha_{\mathrm{gas}} = 0.1\alpha_{-1}$, $\beta = 0.1\beta_{-1}$, $\eta = 0.1\eta_{-1}$, $M = 10^6 M_6 M_\odot$, and $\theta = 0.2\theta_{0.2}$.

We calculate the disk scale height-to-radius ratio $h/r = \Sigma/r\rho$. For the fiducial choice of parameters $\alpha_{-1} = \beta_{-1} = \eta_{-1} = \lambda = \dot{m} = M_6 = q = \theta_{0.2} = 1$, the disk is marginally geometrically thick at the inner edge. We ignore horizontal and vertical advection but do provide an estimate of the advected-to-radiated heat flux ratio $\mathcal{Q}_{\mathrm{adv}}/\mathcal{Q}_{\mathrm{rad}}$. Ignoring radiative loss, we find the advected flux equals $\mathcal{Q}_{\mathrm{adv}} = (3/4)(4\gamma_p - 12\gamma_{\mathrm{T}})\nu\Sigma P_{\mathrm{rad}}/\rho r^2$, where $\gamma_{\rho,T} \equiv d\ln(\rho,T)/d\ln r$; in our disk, $(4\gamma_p - 12\gamma_{\mathrm{T}}) \sim 8$. In the fiducial disk, horizontal advection is competitive with radiative diffusion, implying that the true disk is geometrically thinner than ours, as in the "slim-disk" solutions of Abramowicz et al. (1988). Just how large could the parameter $\dot{m}$ be? The disk must be thin at the edge $(h/r)_{\mathrm{edge}} \ll 1$, implying (we ignore the weak dependence on α, M, and μ)

$$\dot{m} \ll 1.4\beta_{-1}^{0.39}\eta_{-1}\lambda^{1.56}[4q/(1+q)^2]^{0.39}\theta_{0.2}^{-0.49}, \qquad (4)$$

which allows for $\dot{m} \gg 1$ when $q \ll 1$. A trustworthy disk model should also be gravitationally stable, with $Q \equiv \Omega^2/\pi G\rho > 1$ throughout. We have checked that the disk structures for $M \leq 10^6 M_\odot$ have $Q > 1$ inside the radius where T falls below 10^4 K and the disks become susceptible to ionization instability. We do not extrapolate our disks beyond this radius.

3. DETECTION OF THE ELECTROMAGNETIC AFTERGLOW

The pre-coalescent circumbinary disk is expected to be luminous in IR with a negligible X-ray counterpart (Figure 1). Unfortunately, this IR source may be confused with the light of the host galaxy. Barth et al. (2004) recently studied the dwarf galaxy POX 52, which appears to contain a $1.6 \times 10^5 M_\odot$ black hole accreting at about the Eddington rate (Greene & Ho 2004 list other similar candidates). The optical luminosity of the POX 52 black hole is about the same as that of the galaxy, so it seems unlikely that the MBH binary can be identified electromagnetically before the merger.

The black holes merge $t_{\mathrm{gr}}/4$ after decoupling, where t_{gr} is evaluated at decoupling. The gravitational wave losses during

TABLE 1. DISK AT DECOUPLING[a]

Variable	Factor	α_{-1}	$\eta_{-1}/\dot{m}$	λ	M_6	$\beta_{-1}, \frac{4q}{(1+q)^2}$	$\theta_{0.2}$
$a/(GM/c^2)$	117	-0.34	0.24	0.70	0.08	0.42	-0.08
$T\ (10^6\ \mathrm{K})$	1.7	0.19	-0.86	-1.95	-0.28	-0.49	0.30
t_{sh} (yr)	9.4	-1.36	0.98	2.80	1.32	1.7, 0.7	-0.34
h/r	0.46	0.76	-2.43	-3.80	-0.12	-0.95	1.19
$P_{\mathrm{rad}}/P_{\mathrm{gas}}$	2600	1.67	-4.25	-7.35	-0.04	-1.84	2.17
$\kappa_{\mathrm{es}}/\kappa_{\mathrm{abs}}$	46,000	1.76	-4.68	-8.32	-0.18	-2.08	2.32
$Q\ (10^5)$	4.5	2.12	-2.41	-6.61	-1.44	-1.65	1.53
$\mathcal{Q}_{\mathrm{adv}}/\mathcal{Q}_{\mathrm{rad}}$	0.44	1.52	-4.86	-7.60	-0.24	-1.90	2.38
$\epsilon\ (10^{-3})$	1.4	-0.84	2.37	4.20	0.08	1.05	-0.21
$M_{\mathrm{disk}}\ (M_\odot)$	96	-1.17	-0.88	-1.15	2.04	0.21	-0.04

[a]Variable in column 1, defined in the text, equals the factor in column 2 times the product of column head parameters raised to the exponents indicated in columns 3–8, where we assume $\mu = 0.6$. All quantities except for M_{disk} are evaluated at the edge of the disk.
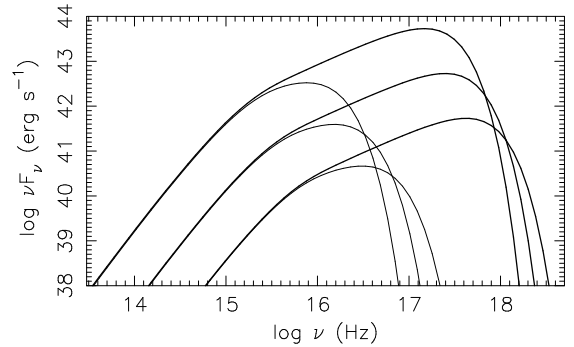

FIG. 1.— Representative thermal disk spectra before the coalescence (*thin lines*) and after (*thick lines*). The spectra are modified blackbody spectra of Eddington-limited ($\dot{m} = 1$) accretion disks around black holes of mass $M = (10^4, 10^5, 10^6)M_\odot$ (*from right to left*) and dimensionless spin parameter $a_* = 0.9$ (we ignored Doppler broadening). Only the emission from rings in the disk with $r < 1000GM/c^2$ was taken into account. These crude spectra are compatible with detailed models of Hubeny et al. (2001). We do not show thermal emission from any accretion disks around individual black holes that may be fed by the gas flow crossing the hollowed region.

merger immediately perturb the potential in which the surrounding gas orbits, giving a (weak) prompt EM signature. Subsequently, the inner edge of the accretion disk migrates inward on timescale $\sim t_{\mathrm{sh}} \sim t_{\mathrm{gr}}$, arriving at the merged black hole $\sim \frac{3}{4}t_{\mathrm{sh}}$ after the merger. Its arrival is accompanied by rapid accretion and the activation of an X-ray active galactic nucleus (AGN). We consider these two distinct types of EM signatures in turn.

The few percent reduction in the total black hole mass due to gravitational wave losses excites a weak axisymmetric wave in the disk. More interestingly, the coalescence may be accompanied by radiation recoil (e.g., Merritt et al. 2004, and references therein). The velocity of the recoiled black hole, $v_{\mathrm{rec}} \lesssim 300$ km s^{-1}, is much smaller than the orbital velocity of the disk at the inner edge, $\sim 2 \times 10^4$ km s^{-1}. Disk material at radius r remains entirely bound to the black hole if its orbital velocity prior to the recoil $(GM/r)^{1/2}$ is larger than $\sim 2.4v_{\mathrm{rec}}$, which is true for the inner disk. The recoil drives waves and warps in the outer disk. If these result in shocks or obscuration, they could result in an observable EM signature.

More certain is the afterglow due to the viscous migration of the inner edge of the disk and consequent turn-on of X-ray emission from a rapidly accreting AGN. *LISA* will de-
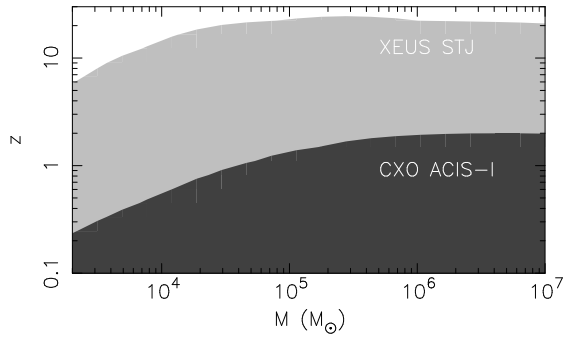
FIG. 2.— Redshifts at which emission from an Eddington-accreting ($\dot{m} = 1$) black hole of mass M can be detected with 10^5 s exposure using the instrument ACIS-I on *Chandra* (*dark gray*) and the Hafnium superconducting tunneling junction (STJ) detector on XEUS before mission upgrade (light-grey). We assume that 10 counts constitute detection and ignore absorption and confusion. The disk spectra were thermal modified blackbody spectra for a nearly maximally spinning black hole, $a_* = 0.9$. We assume the standard ΛCDM cosmology with $H_0 = 70$ km s^{-1} Mpc^{-1}, $\Omega_{\rm m} = 0.3$, and $\Omega_\Lambda = 0.7$.

tect with a high signal-to-noise ratio the coalescence of black holes with masses $(10^5 - 10^7)(1 + z)^{-1} M_\odot$ at redshifts $z \lesssim 20$. Can the EM afterglow also be detected? From Table 1, we estimate the observed interval $\Delta t \sim \frac{3}{4}(1 + z)t_{\rm sh}$ between the two signals. For example, for the merger of two $10^5 M_\odot$ black holes at $z = 5$, assuming $\alpha_{-1} = \beta_{-1} = \eta_{-1} = \dot{m} = \theta_{0.2} = 1$, we find $\Delta t \sim 2$ yr for a graybody disk truncated at $r_{\rm edge} = 2a$. A strong recoil could shorten this. Most of the luminosity of the post-coalescent accretion disk around a $(10^4 - 10^6) M_\odot$ black hole is emitted at rest-frame energies $h\nu \sim (0.5 - 5)$ keV (see Figure 1), which fall within the sensitivity windows of future X-ray detectors such as *XEUS*[3] and *Generation-X*.[4] *XEUS* could

see this emission at $z \sim 20$ for $\gtrsim 10^5 M_\odot$ black holes. For smaller black holes, the maximum redshift for detection decreases with the decreasing mass (see Figure 2).

At $z \lesssim 20$, the *James Webb Space Telescope*[5] is sensitive to rest-frame mid-UV to near-IR, which come from the disk radii exterior to the inner edge at decoupling (Figure 1). Therefore, the post-coalescence IR–optical flux will not be very different from the pre-coalescence flux. An exception would be if the merged black hole were enshrouded by a large column depth of gas and dust. Then, the UV–X-ray emission would be reprocessed to longer wavelengths. Such a shrouded merger could be identified by a sudden increase in IR luminosity.

We therefore propose that locations with detected GR signals from MBH coalescence be monitored in the $0.1 - 10$ keV band at high angular resolution. The angular resolution of *LISA* ranges from several arcminutes to several degrees depending on the black hole mass, mass ratio, and redshift (Cutler 1998; Hughes 2002). Therefore, multiple exposures of an X-ray telescope may be necessary for some sources. A possibly confusing source of X-ray flares are tidal disruptions of mainsequence stars (Rees 1990; Cannizzo, Lee, & Goodman 1990; Komossa et al. 2004). Detection of the afterglow of MBH coalescence will help pinpoint the location and hence redshift of GR sources. The detailed light curve of the afterglow will probe the structure of the accretion disk as it moves toward the black hole, and will also shed light on the cosmological assembly of MBHs.

[3] http://www.rssd.esa.int/index.php?project=XEUS.
[4] http://generation-x.gsfc.nasa.gov.
[5] http://www.stsci.edu/jwst.

REFERENCES

Abramowicz, M. A., Czerny, B., Lasota, J. P., & Szuszkiewicz, E. 1988, ApJ, 332, 646
Armitage, P. J. & Natarajan, P. 2002, ApJ, 567, L9
Artymowicz, P. & Lubow, S. H. 1994, ApJ, 421, 651
Artymowicz, P. & Lubow, S. H. 1996, ApJ, 467, L77
Balbus, S. A. & Hawley, J. F. 1991, ApJ, 376, 214
Bardeen, J. M. & Petterson, J. A. 1975, ApJ, 195, L65
Barth, A. J., Ho, L. C., Rutledge, R. E., & Sargent, W. L. W. 2004, ApJ, 607, 90
Begelman, M. C. 2002, ApJ, 568, L97
Begelman, M. C., Blandford, R. D., & Rees, M. J. 1980, Nature, 287, 307
Cannizzo, J. K., Lee, H. M., & Goodman, J. 1990, ApJ, 351, 38
Cutler, C. 1998, Phys. Rev. D, 57, 7089
Gammie, C. F. 1998, MNRAS, 297, 929
Greene, J. E. & Ho, L. C. 2004, ApJ, 610, 722
Greenhill, L. J., et al. 2003, ApJ, 590, 162
Günther, R., Schäfer, C., & Kley, W. 2004, A&A, 423, 559
Hubeny, T., Blaes, O., Krolik, J. H., & Agol, E. 2001, ApJ, 559, 680
Hughes, S. A. 2002, MNRAS, 331, 805
Ivanov, P. B., Papaloizou, J. C. B., & Polnarev, A. G. 1999, MNRAS, 307, 79
Jackson, J. M., Geis, N., Genzel, R., Harris, A. I., Madden, S., Poglitsch, A., Stacey, G. J., & Townes, C. H. 1993, ApJ, 402, 173

Komossa, S., Halpern, J., Schartel, N., Hasinger, G., Santos-Lleo, M., & Predehl, P. 2004, ApJ, 603, L17
Larwood, J. D. & Papaloizou, J. C. B. 1997, MNRAS, 285, 288
Lightman, A. P. & Eardley, D. M. 1974, ApJ, 187, L1
Liu, F. K., Wu, X., & Cao, S. L. 2003, MNRAS, 340, 411
Lubow, S. H., Seibert, M., & Artymowicz, P. 1999, ApJ, 526, 1001
Lynden-Bell, D. & Pringle, J.E. 1974, MNRAS, 168, 603
Merritt, D., Milosavljević, M., Favata, M., Hughes, S. A., & Holz, D. E. 2004, ApJ, 607, L9
Miller, K. A. & Stone, J. M. 200, ApJ, 534, 398
Milosavljević, M. & Merritt, D. 2003, ApJ, 596, 860
Miyoshi, M., Moran, J., Herrnstein, J., Greenhill, L., Nakai, N., Diamond, P., & Inoue, M. 1995, Nature, 373, 127
Peters, P. C. 1964, Physical Review , 136, 1224
Pringle, J. E. 1991, MNRAS, 248, 754
Rees, M. J. 1990, Science, 247, 817
Sakimoto, P. J. & Coroniti, F. V. 1981, ApJ, 247, 19
Shakura, N. I. & Sunyaev, R. A. 1973, A&A, 24, 337
Turner, N. J. 2004, ApJ, 605, L45
Turner, N. J., Stone, J. M., Krolik, J. H., & Sano, T. 2003, ApJ, 593, 992